Article

Not peer-reviewed version

Novel Strategy for Surface Modification of Titanium Implants towards the Improvement of Osseointegration Property and Antibiotic Local Delivery

Isabela da Rocha Silva , Aline Tavares da Silva Barreto , Renata Santos Seixas , Paula Nunes Guimarães Paes , Juliana do Nascimento Lunz , Rossana Mara da Silva Moreira Thiré * , Paula Mendes Jardim *

Posted Date: 27 February 2023

doi: 10.20944/preprints202302.0449.v1

Keywords: titanium; hydrothermal treatment; surface modification; local drug delivery system; osseointegration

Article

Novel Strategy for Surface Modification of Titanium Implants towards the Improvement of Osseointegration Property and Antibiotic Local Delivery

Isabela da Rocha Silva[1], Aline Tavares da Silva Barreto[2], Renata Santos Seixas[1], Paula Nunes Guimarães Paes[3], Juliana do Nascimento Lunz[4], Rossana Mara da Silva Moreira Thiré[1*] and Paula Mendes Jardim[1*]

[1] COPPE/Program of Metallurgical and Materials Engineering – PEMM, Universidade Federal do Rio de Janeiro – UFRJ, Rio de Janeiro RJ, Brazil; draisabelarocha@gmail.com; renata_ss@msn.com; rossana@metalmat.ufrj.br; pjardim@metalmat.ufrj.br

[2] Graduation Program in Nanobiosystems, Universidade Federal do Rio de Janeiro - UFRJ, Duque de Caxias RJ, Brazil; alinetsb@nano.ufrj.br

[3] Faculdade de Odontologia, Universidade do Estado do Rio de Janeiro - UERJ, Rio de Janeiro RJ, Brazil; paes.paula@ce.uerj.br

[4] Divisão de Metrologia de Materiais, Instituto Nacional de Metrologia, Qualidade e Tecnologia - Inmetro, Xerém RJ, Brazil; jnlunz@gmail.com

* Correspondence: RMSMT: rossana@metalmat.ufrj.br; PMJ: pjardim@metalmat.ufrj.br; Tel.: +55 21 3938-8500

Abstract: The topography and chemical composition modification of the titanium (Ti) implants play a decisive role in improving biocompatibility and bioactivity, accelerating osseointegration, and, thus, determining clinical success. In spite of the development of surface modification strategies, bacterial contamination is a common cause of failure. The use of systemic antibiotic therapy does not guarantee action at the contaminated site. In this work, we proposed a surface treatment for Ti implant that aim to improve its osseointegration and reduce bacterial colonization in surgery site due to local release of antibiotic. The Ti disks were hydrothermally treated with 3M NaOH solution to form a nanostructured layer of titanate on the Ti surface. Metronidazole was impregnated on these nanostructured surfaces to allow its local release. The samples were coated with poly(vinyl alcohol) - PVA films with different thickness to evaluate a possible control of drug release. Gamma irradiation was used to crosslink the polymer chains leading to a hydrogel layer formation and to sterilize the samples. The samples were characterized by XRD, SEM, FTIR, contact angle measurements, "in vitro" bioactivity, and drug release analysis. The alkaline hydrothermal treatment successfully produced intertwined, web-like nanostructures on the Ti surface, providing wettability and bioactivity to Ti samples (Ti+TTNT samples). Metronidazole was successfully loaded and released from Ti+TTNT samples coated or not with PVA. Although the polymeric film acted as a physical barrier to drug delivery, all groups reached the minimum inhibitory concentration for anaerobic bacteria. Thus, the surface modification method presented is a potential approach to improve the osseointegration of the Ti implant and to associate local drug delivery to dental implants, preventing early infections and bone failure.

Keywords: titanium; hydrothermal treatment; surface modification; local drug delivery system; osseointegration

1. Introduction

Titanium implants are a safe and predictable alternative for rehabilitation treatments in dental surgeries, and their success is related to osseointegration. Titanium is considered as the material of choice for the manufacture of implants due to its mechanical properties, chemical stability, and biocompatibility [1,2]. Surface treatments such as alkaline hydrothermal treatment have been developed and improved to modify and optimize the physical-chemical properties of the surface, such as roughness, topography,

 doi:10.20944/preprints202302.0449.v1

wettability, and its composition, influencing cellular events during the healing process [3,4]. Such treatment allows the growing of layer of titanate nanostructures on Ti surface, which increases the roughness and consequently the surface area, and hydrophilicity, favoring protein adsorption and cell adhesion and proliferation [4]. The morphology of nanostructures is directly dependent on the experimental conditions used for hydrothermal treatment.

Infections associated with the surgical procedures during dental implantation are one of the causes of osseointegration failure, leading to its loss [5]. Such infections can be caused by contamination of bacteria that already exist at the surgical site, especially in patients with pre-existing periodontal disease [6]. The most critical moment, regarding early loss induced by infection, is when the implant comes into contact with human cells and local microorganisms in the initial moments after its installation [7]. Prophylactic antibiotic therapy has been proposed to decrease bacterial levels at the site to be instrumented. The pre-established biofilm restricts the diffusion of molecules and bacterial sensitivity to antibiotics, making the systemic prophylactic antibiotic therapy not having the desired effectiveness [8]. Therefore, it is desirable to develop strategies with a local antibiotics release approach as an alternative to systemic oral antimicrobial therapy. The use of biodegradable material in combination with titanium implants as a local drug delivery system is an interesting approach.

Hydrogels have gained considerable attention in recent years for their unique physical-chemical properties, similar to those of living tissues, such as high water content, soft and rubbery consistency, low interfacial tension with water or biological fluids [9]. These materials can be defined as a 3D network formed from physical or chemical crosslinked, hydrophilic polymers. They can swell in contact with water or biological fluids without losing their structural integrity [10]. Poly(vinyl alcohol) hydrogels (PVA) have been recognized as promising biomaterials and suitable candidates for drug delivery systems [11]. PVA is a biodegradable, biocompatible, non-toxic, and water-soluble polymer.

Metronidazole is an antibacterial compound belonging to the class of imidazoles, a subgroup of nitroimidazoles, which acts against a wide variety of microorganisms. It is clinically effective in the treatment of periodontitis and peri-implantitis caused by anaerobic bacteria [12]. It presents a good therapeutic response, but its high toxicity after continuous systemic doses can, for example, manifest gastrointestinal disorders, dizziness, headaches, among others, often causing the patient to discontinue treatment [13]. Thus, a local delivery of metronidazole could reduce the systemic toxicity of the antibiotic and increase its efficiency even with lower dose.

In the present work, we propose a surface treatment methodology to titanium implant aiming to provide antimicrobial property by local release of metronidazole and improvement of osseointegration capacity obtained by nanostructures incorporation on the titanium surface. The proposed system consists of Grade 4 Ti sample functionalized with a nanostructured titanate layer, which was produced by hydrothermal treatment, impregnated with metronidazole and coated by PVA hydrogel to control the antibiotic release. Grade 4 Ti has been the industry standard for dental implants for years due to its high strength and low malleability. The great advantage of surface modification is to modify of few external layers of the materials without affecting its bulky characteristics, such as mechanical properties. In other words, it is possible to change biomaterial-cells interaction without changing bulky physical and chemical properties.

2. Materials and Methods

2.1. Preparation of titanate nanostructured coating

Grade 4 Ti disks were used in the alkaline hydrothermal treatment as a substrate surface for growing titanate layer. Prior treatment, the Ti disks (12 mm diameter and 2 mm thickness) were mechanically polished with silicon carbide abrasive papers of different grades (220, 400, 600 e 1500), and then ultrasonically cleaned for 10 minutes with

Preprints (www.preprints.org) | NOT PEER-REVIEWED | Posted: 27 February 2023 doi:10.20944/preprints202302.0449.v1

acetone, ethanol and distilled water sequentially. The alkaline hydrothermal treatment was conducted in a high pressure reactor (BR-500 – Berghof) under a 3M NaOH solution at 150°C for 6 hours. After synthesis reaction, the samples were washed by distilled water immersion four times for 10 minutes, as will be described below.

2.2. Loading of metronidazole in nanostructures

Metronidazole (MNZ) (0.5% (m/v) metronidazole injection solution, Fresenius Kabi Brasil Ltda.) was added to the coated Ti disks to interact with the nanostructures and to compose the drug delivery system. First, 25 μL-drop of MNZ was pipetted on to disks and allowed to dry at room temperature. After drying, another drop was added. This procedure was repeated eight times until 22.2 μg/mL of MNZ was deposited. In the case of systems with thicker layer of PVA coating, it was necessary to deposit higher volume of MNZ (33.3 μg/mL) in order to maintain the released amount of MNZ within the range of the sensitivity of the method.

2.3. Polymeric coating of nanostructured samples

Poly(vinyl alcohol) (PVA) (Mw 85.000–124.000 g/mol, degree of hydrolysis >99%, Sigma-Aldrich) was used to coat the MNZ-loaded samples to control the drug release. For the production of PVA films, PVA was dissolved in distilled water at 90 ± 2°C for 4 hours under magnetic stirring to obtain 10% (m/v) PVA aqueous solution. Then, the solution was cooled under stirring to 50°C and 0.2 ml of PVA solution was pipetted onto the samples. Spin coating technique was performed at a rotational speed of 400 rpm for 10 seconds, followed by a rotational speed of 4000 rpm for 60 seconds, to ensure even coverage. Two different groups were produced by this procedure for comparative purposes, a group with one layer and with six layers of polymeric coating. After the coating procedure, all the samples were left in a ventilated oven for 20 h at 50 °C.

2.4. Crosslinking of polymeric coating

In order to crosslink the polymeric films, PVA-coated samples (TTNT+MNZ+1PVA, TTNT+MNZ+6PVA groups) were irradiated with gamma rays of Cobalt-60 at a dose of 25 KGy. By using this procedure, samples can be sterilized concomitantly with PVA chains crosslinking [14]. The experimental groups were named as shown in Table 1.

Table 1. Experimental groups.

Groups	Description
TTNT	Titanate nanostructures on Ti disk surface via hydrothermal synthesis
TTNT+MNZ	Titanate nanostructures on Ti disk surface via hydrothermal synthesis + Metronidazole
TTNT+MNZ+1PVA	Titanate nanostructures on Ti disk surface via hydrothermal synthesis + Metronidazole + 1 layer of irradiated PVA film
TTNT+MNZ+6PVA	Titanate nanostructures on Ti disk surface via hydrothermal synthesis + Metronidazole + 6 layers of irradiated PVA film

2.5. Microstructural characterization

The sample after hydrothermal treatment was analyzed by Grazing Incidence X-ray diffraction (GIXRD) and Scanning Electron Microscopy (SEM). The GIXRD (X'pert PRO/PANalytical) patterns were collected using CuKα radiation (λ= 1.5418 Å) and incidence angle of the beam in relation to the samples surface of 1º. The surface morphology of the samples was examined using SEM (Versa 3D/Thermo Fisher, Helios/Thermo Fisher and Vega/Tescan). The chemical bonds of the samples were analyzed by FTIR spectrometer (Nicolet 6700, Thermo Scientific) equipped with ATR (Attenuated Total Reflection)

Preprints (www.preprints.org) | NOT PEER-REVIEWED | Posted: 27 February 2023 doi:10.20944/preprints202302.0449.v1

accessory and using resolution of 4 cm-1 in the region of 4000–650 cm-1. The signal of the obtained spectra was processed with Origin Pro version 9.1 software using the Savizky-Golay algorithm (five smoothing points) and normalized to [0, 1].

2.6. Apatite deposition – "In vitro" Bioactivity Assay

The samples were soaked in simulated body fluid (SBF) to assess their bioactivity by examining calcium phosphate crystals formation on the surface. SBF was prepared according to Kokubo's formulation and the bioactivity test was performed in accordance with ISO/FDIS 23317 (Implants for surgery — In vitro evaluation for apatite-forming ability of implant materials). Alkaline hydrothermally treated Ti samples and untreated Ti (control sample) were soaked in SBF at pH=7.4 and constant temperature of 36.5 ºC for 14 days. After soaking period, the samples were gently washed with distilled water and dried in a desiccator at room temperature. The formation of calcium phosphate crystals after soaking period was investigated by means of SEM (Vega/Tescan) and GIXRD (X'pert PRO/PANalytical). The samples were gold-coated prior to SEM analysis.

2.7. "In vitro" drug release

The release of metronidazole from the samples was investigated for 14 days by immersion in 45 mL of phosphate-buffered saline (PBS, pH 7.4, composition: 8.0 g NaCl, 1.1 g Na_2HPO_4, 0.2 g KCl, 0.2 g KH_2PO_4) at 37 °C and rotational speed of 100 rpm. Measurement of the initial release was performed after 20 min of immersion, followed by 1; 1.8 ; 24; 48; 96; 168; 216; 264 and 336 h. At each interval, 4 mL of PBS was withdrawn, and the same fresh amount was replaced. In order to disregard the effects of this dilution, the following mathematical correction was made:

$$Correction\ Factor = \left(\frac{45}{45-4}\right)^{n-1}$$

Where n is the sequential number of the sample, 45 is the volume in milliliters of the PBS solution and 4 is the volume in milliliters of the removed aliquot. To perform the correction, the volume of antibiotic release measured in the spectrophotometry was multiplied by this factor [15].

The amount of drug released was measured by Ultraviolet/Visible Spectroscopy (UV/Vis) equipment (mod. SP-220, Biospectro). To determine the concentrations of the metronidazole in collected solution, a standard curve of absorbance at wavelength 320 nm versus known concentrations was used.

The surface of samples before and after the drug release experiment was analyzed by SEM.

2.8. Statistical analysis

The MNZ release data were analyzed using a commercially available statistical program (SigmaPlot for Windows version 11.0). Data are reported as mean ± standard deviation. If the difference was determined to be significant after the analysis of variance, pairwise comparisons were performed using a Holm-Sidak post-hoc test, and $p < 0.05$ was considered statistically significant. The experiment was performed with all readings for each point of the release done in triplicate.

3. Results and Discussion

3.1. Titanate nanostructured coating

The speed and quality of osseointegration are directly linked to the surface roughness and chemical composition created in the titanium. Surface treatments such as alkaline hydrothermal modifies the topography of titanium on a nanoscale [16] to generate a surface that accommodates host cells, promoting an environment conducive to cell growth and enhancing the osseointegration process [17]. Besides that, the presence of

 doi:10.20944/preprints202302.0449.v1

Na+ ions on the titanate surface plays an important role in the apatite formation and therefore its bioactivity [18,19]. The alkaline hydrothermal treatment consists of submerging the sample in an alkaline solution under certain conditions of high temperature, pressure and time to form a titanate layer with nanoscale architecture [16]. The topography resulting from this process is determined by the combination of these parameters, being attractive due to its simplicity, cost-effectiveness and potential for large-scale manufacturing [16,20].

Fig.1 shows a comparison of SEM images from the top view of the Ti surface before and after the alkaline hydrothermal treatment under the proposed conditions (3M NaOH, 150°C, 6 h). The hydrothermal synthesis condition chosen was based on a work by this group to be published, in which the bioactivity of different microstructures was evaluated. The Ti surface before hydrothermal treatment shows parallel grooves produced by polishing without any specific nanoscale topography (Fig. 1a). On the other hand, the sample surface after treatment presented a microstructure composed by intertwining of nanofibers with approximately 83 nm in diameter, giving rise to micropores with at about 500 nm in size. This web-like morphology resembles that of extracellular matrix of bone tissue, which can stimulate cell adhesion, proliferation and differentiation.

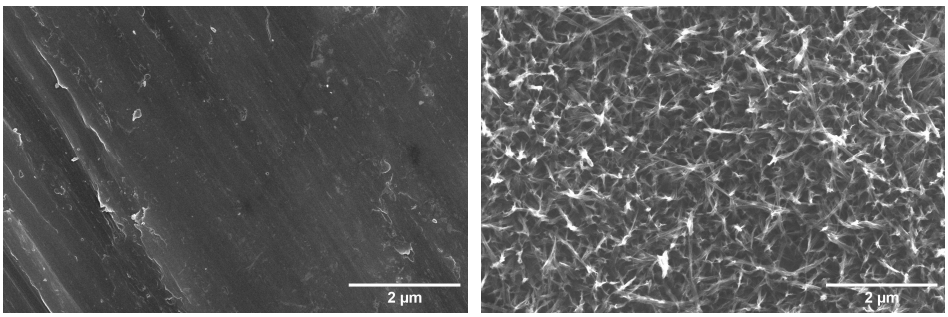

(a) (b)

Figure 1. Top-view SEM image of Ti surface before (a) and after (b) alkaline hydrothermal treatment.

Bone healing around an implant begins through cellular communication. Bone marrow mesenchymal cells interact with the implant surface and surface properties, such as morphology, wettability, mechanical and chemical properties, influence this process. Thus, the implant must function as a bioactive and biocompatible scaffold, with osteogenic characteristics that enable the migration, adhesion and proliferation of cells of the osteogenic lineage. The presence of a nanoscale framework that allows vascular proliferation and the passage of signaling molecules induces a desired cellular response, since interactions between cells and biomaterials occur at the nanoscale. Titanium surfaces hydrothermally treated with sodium hydroxide produce a nanoporous architecture that promotes appropriate cellular interaction with the surface promoting the osteoblastic lineage [17].

The formation of titanate layer was also confirmed by Grazing Incidence X-ray Diffraction (GIXRD). This is a surface sensitive technique that utilizes a small incident angle X-ray beam, being very useful to analyze crystalline microstructure of thin films. Fig. 2 shows the GIXRD pattern of the resulting nanostructured film, revealing typical diffraction peaks of layered sodium titanate, especially that peak at $2\theta \sim 10°$, attributed to the distance between layers [21]. The peaks at $2\theta = 35.2°$, 38.6°, 40.3°, 53.2°, 63.1° and 70.8 ° correspond to the Ti substrate.

Preprints (www.preprints.org) | NOT PEER-REVIEWED | Posted: 27 February 2023 doi:10.20944/preprints202302.0449.v1

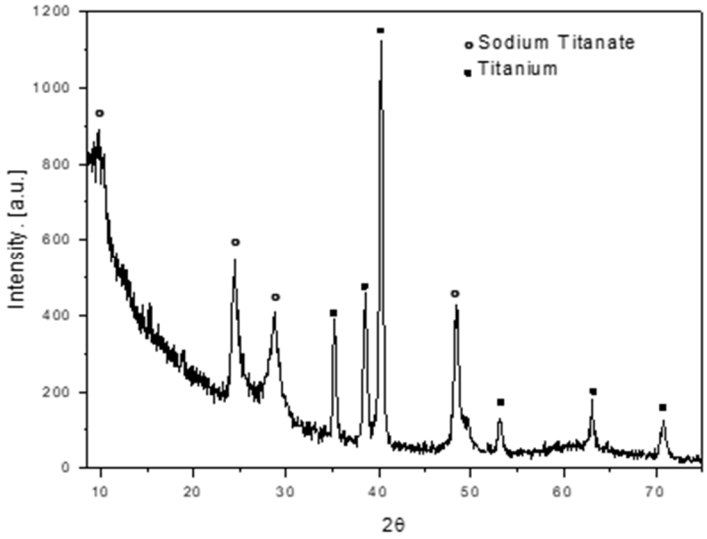

Figure 2. GIXRD diffractogram of Ti surface after hydrothermal treatment (TTNT).

3.2.". In vitro" bioactivity assay

When an artificial material is implanted in a living body, it can be consider a bioactive material if it is able to connect to the living bone through a thin layer rich in calcium and phosphorous (apatite layer) without a disstinct boundary. According to ISO/FDIS 23317 Standard, the formation of a bone-like apatite layer can be "in vitro" reproduced when a material is immersed in an acellular and protein-free simulated body fluid (SBF) with ion concentrations nearly equal to those of human blood plasma. Thus, under this condition, the formation of apatite layer on the material surface is an indicative of its in vivo bone-bonding ability.

In Fig.3, SEM images of the surface of Ti disks with (TTNT) and without hydrothermal treatment after 14 days of incubation in SBF solution (pH 7.4, 37°C). The uniform layer of the flake-like apatite crystals can only be identified covering the sodium titanate structure (Fig. 3b). The apatite formation capacity of Ti disks submitted to hydrothermal treatment can be explained by the exchange of titanate Na+ ions with H3O+ ions in the SBF solution to form a Ti-OH bond on the surface. In response, the surface becomes negatively charged, which reacts with the calcium ions present in the SBF. These Ca+ ions are accumulated, making the surface positively charged and reacting with the negatively charged phosphate ions, which causes an increase in the rate of apatite nucleation [18,19].

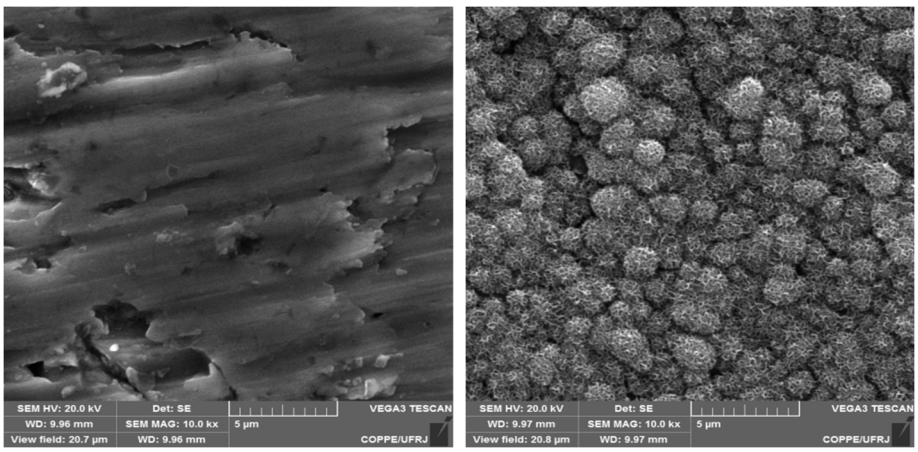

(a) (b)

Figure 3. SEM images of samples surface after 14 days of bioactivity test comparing polished Ti without (a) and with alkaline hydrothermal treatment, TTNT (b).

Preprints (www.preprints.org) | NOT PEER-REVIEWED | Posted: 27 February 2023 doi:10.20944/preprints202302.0449.v1

Figure 4 shows the GIXRD diffractograms of Ti hydrothermally treated (TTNT) before and after immersion in SBF. The typical peaks of apatite at 2θ = 26° and 2θ = 32° (ICSD 9-432) was observed only in the diffractogram of TTNT after immersion in SBF, confirming the formation of an uniform layer of apatite on TTNT surface and thus, indicating that the hydrothermal treatment provide bioactivity to Ti samples.

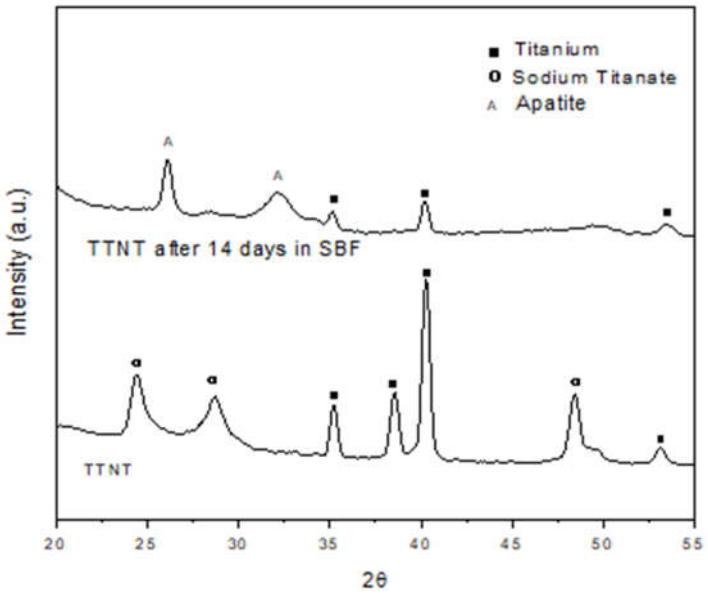

Figure 4. Diffractograms of Ti hydrothermally treated surface before and after immersion in SBF for 14 days.

3.2. Surface wettability

Wettability influences the cascade of biological events that initiate osseointegration [22]. A hydrophilic surface results in closer contact of the titanium surface with the blood clot and cells by means of increased availability of serum proteins with binding energy. The increase in cell adhesion capacity by these proteins improves the adherence of the fibrin network and its retention to the surfaces of implants, as they mediate cell adhesion, followed by the cascade of coagulation and migration of undifferentiated cells and osteoblastic precursors [22,23].

Fig. 5 presents the images of a water droplet obtained during the contact angle measurements to evaluate the modification of surface wettability due to the surface treatment of Ti disks. In this context, the experimental group TTNT + MNZ + 1PVA was subjected to the analysis of the contact angle (Fig.5c) to monitor the change in wettability suffered after deposition of the PVA layer when compared to Ti pure samples (Fig.5a) and Ti samples after hydrothermal treatment (TTNT, Fig.5c).

Preprints (www.preprints.org) | NOT PEER-REVIEWED | Posted: 27 February 2023 doi:10.20944/preprints202302.0449.v1

(a) (b) (c)

Figure 5. Contact angle measurements. Images of a water droplet on the surface of (a) pure Ti surface, (b) Ti disk after alkaline hydrothermal treatment (TTNT), (c) Ti disk after addition of metronidazole (MNZ) and a layer of PVA (TTNT + MNZ + 1PVA).

The contact angle of the water drop on the surface of the pure titanium samples presented the highest value (θ_c = 46°), indicating the less hydrophilic character of these samples. After the hydrothermal treatment, the water droplet spreads out on the TTNT surface, showing a superhydrophilic behavior (θ_c = 0°). This could be explained considering the increase in the surface area and the pores formation due to the presence of titanate layer, so that the decrease in contact angle may be related to the drop absorption by capillarity. Additionally, although PVA molecules present a hydrophilic character, the contact angle value increased a little after MNZ addition and PVA coating. However, TTNT + MNZ + 1PVA samples also presents high hydrophilic character with θ_c = 22°. This fact could be explained by the smoothing of surface roughness by the coating with PVA layer, which probably hindered the water absorption by capillarity through the TTNT nanostructures. The hydrophilicity of the drug delivery system after PVA deposition for osseointegration purposes is important and indicates that this coated device could play a positive and significant role in the early stages of osseointegration.

3.3.". In vitro" metronidazole release evaluation

For osseointegration to occur, four stages are required: hemostasis, inflammatory phase, proliferative phase, and remodeling phase, which must occur in a coordinated and organized manner [24,25], resulting in impeccable healing. The misalignment of this healing can occur in the initial inflammatory phase, which begins about 10 minutes after the implant is installed, creating a toxic environment. Host defense systems are activated at this stage by nonspecific molecules of bacterial origin. Polymorphonuclear leukocytes (PMN) and macrophages, and a group of glycoproteins that form membrane-perforating channels (perforins), which damage bacterial cells, are activated [26]. Therefore, the abundance of bacteria, as is the case with patients with active periodontal disease, for example, prolongs and amplifies the cellular immune response. PMNs kill bacteria through reactive radicals (oxygen species and hydroxylated groups, chlorine radicals and hypochlorite) that are also toxic to the host's cells and to the healthy tissue around the wound. Thus, a fulminant neutrophil response can induce the loss of healthy surrounding tissues [26].

To limit the inflammatory phase, antibacterial measures are needed, such as antibiotic therapy and local disinfection. The local and controlled release of the drug directly from the surface of the implant could act to combat bacteria, preventing their adhesion, exacerbating the inflammatory process, and failing the osseointegration process. To propose a release restriction, it was suggested the use of PVA with different number of layers to compare the release in different systems.

Fig. 6 shows the evolution with time of cumulative release of metronidazole from TTNT + MNZ samples with and without PVA coating during their immersion in PBS (pH 7.4, 37°C). Table 2 shows the accumulated percentage of MNZ released during the first 48 hours.

Preprints (www.preprints.org) | NOT PEER-REVIEWED | Posted: 27 February 2023 doi:10.20944/preprints202302.0449.v1

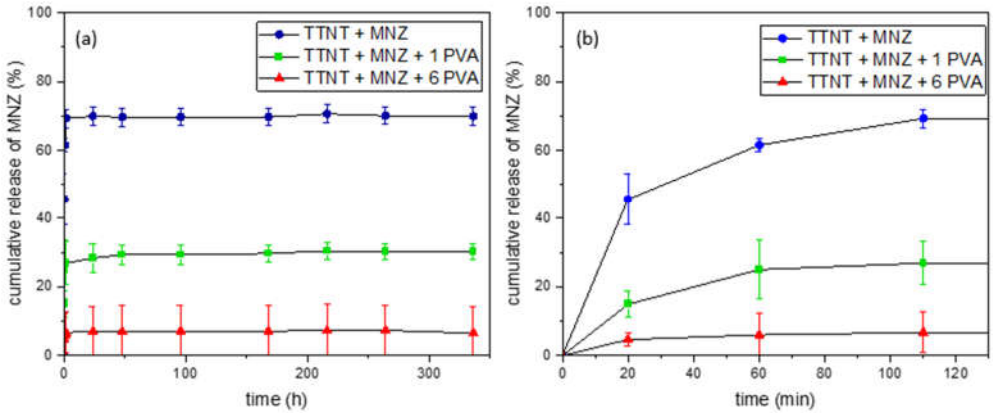

(a) (b)

Figure 6. Cumulative release of MNZ with time: (a) whole experiment (14 days); (b) first 110min.

Table 2. Percentage of MNZ released in each measurement during the assay and statistical difference (different upper-case letters within a column indicate significant differences among experimental groups, different lowercase letters within a row indicate significant differences among time).

% of MNZ released	20 min	60 min	110 min	24 h	48 h
TTNT+MNZ	45.7^{cA}	61.5^{bA}	69.3^{aA}	69.9^{aA}	69.6^{aA}
TTNT+MNZ+1PVA	14.9^{bB}	25.0^{aB}	26.9^{aB}	28.4^{aB}	29.3^{aB}
TTNT+MNZ+6PVA	4.66^{aC}	6.01^{aC}	6.72^{aC}	7.01^{aC}	7.02^{aC}

For all groups, the total amount of MNZ was not released in the medium. The maximum release of the drug was 70%, observed for TTNT + MNZ group. This can be justified by a possible interaction between sodium titanate and metronidazole, which would prevent these molecules from being released by diffusion during the test, a suggestion that was confirmed by FTIR analyses. The samples coated with PVA, TTNT + MNZ + 1PVA and TTNT + MNZ + 6PVA groups, presented a significant reduction in the total percentage of MNZ released, at about 27% and 6%, respectively. For these groups, besides the titanate-metronidazole interaction, PVA coating acted as a physical barrier, limiting the amount of MNZ released.

The hypothesis that there is no difference among group means was rejected by Two Way Repeated Measures ANOVA (One Factor Repetition) that assumed a statistically significant interaction between MNZ released by each experimental group and time. ($p \leq 0.001$). In Table 2, a statistical treatment with all pairwise multiple comparison procedures (Holm-Sidak method) with overall significance level= 0.05 was carried out to observe, in a more reliable way, the difference between the release times, comparing the different groups. According to the data, TTNT + MNZ + 6PVA group reached its release constant in just 20 min, which could be justified by the efficiency of a physical barrier formed by the 6 layers of PVA deposited on the surface. The group TTNT + MNZ + 1PVA had its constant release in 60 minutes, while the sample TTNT + MNZ continues to release until 110 min. These results imply that drug release profile can be designed according to the thickness of PVA coating.

Although the PVA coating did not promote a gradual and prolonged release of MNZ, as expected, the metronidazole concentrations released for all groups (1.6 – 15.5 µg/mL) were higher than the Minimum Inhibitory Concentration (MIC) of this drug for anaerobic bacteria. MIC is the lowest antibiotic concentration needed to destroy specific

Preprints (www.preprints.org) | NOT PEER-REVIEWED | Posted: 27 February 2023 doi:10.20944/preprints202302.0449.v1

bacteria. Previous studies [27] reported the MIC of metronidazole to kill anaerobic bacteria without distinction as 0.06 to 32 μg/mL. Moreover, as discussed before, the local delivery of MNZ in an immediate regime could reduce early implant complication by removing the bacterial contamination of the surgical site and thus, avoiding disturbance in the initial inflammatory phase of wound healing, which begins 10 min after the implantation.

3.4. Chemical composition evaluation after "in vitro" metronidazole release analysis

The samples were analyzed by FTIR before and after the drug release experiment. For a better interpretation of the FTIR spectra of the groups with MNZ, the FTIR spectra of nanostructured Ti samples after alkaline hydrothermal treatment (TTNT) and pure PVA film, shown in Fig.7 and Fig.8 respectively, were previously analyzed.

In the spectrum of TTNT sample (Fig.7), a broad band between 3000 and 3500 cm^{-1} is observed, which can be attributed to fundamental stretching vibrations of different hydroxyl groups O-H (free or linked) [28,29,30]. It may be due to the absorption of water from the atmosphere [29] and the formation of the Ti-OH bond. The band at 1630 cm^{-1} can be attributed to bending vibrations of -OH [28,29] and can indicate water absorption of the titanate when exposed to the atmosphere [30]. The set of overlapping bands in the 800 to 400 cm^{-1} range may be related to the Ti-O and Ti-O-Ti groups [28].

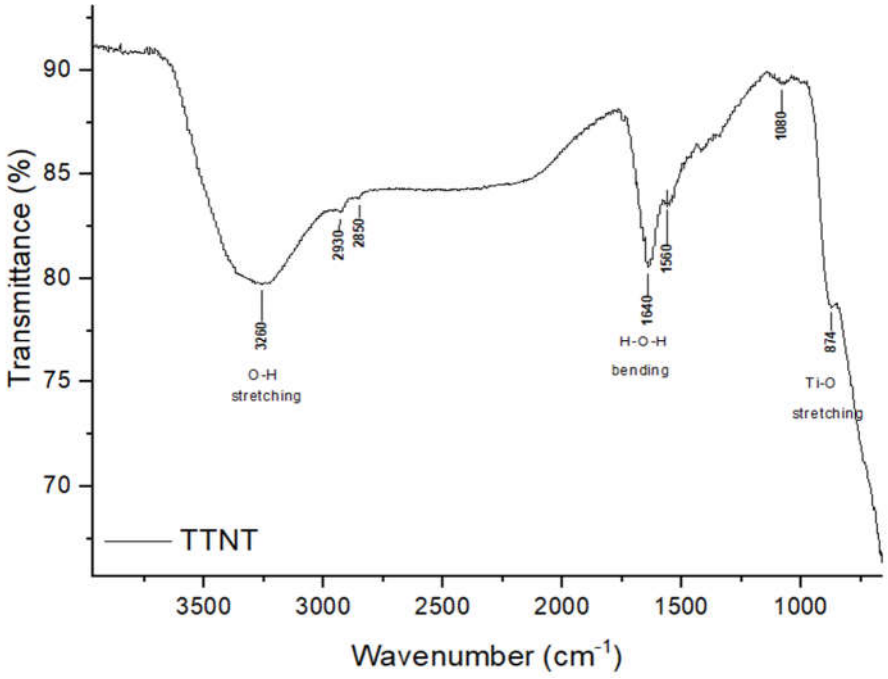

Figure 7. FTIR spectra of Ti sample after alkaline hydrothermal treatment (TTNT).

PVA gamma irradiated film was used as reference in identifying the characteristic absorption bands of TTNT+MNZ coated samples. FTIR spectrum of PVA film (Fig.8) shows the following bands and their respective vibration modes: 3280 cm^{-1}, the hydroxyl group stretching vibration; 2930 cm^{-1} and 2851 cm^{-1}, C–H stretching vibration in CH_2 groups; 1649 cm^{-1} and 1559 cm^{-1}, C=O stretching vibration and C=C stretching vibration, respectively, of the non-hydrolyzed acetate groups; 1414 cm^{-1}, C–H wagging vibration in CH2 groups; 1329 cm^{-1}, (CH+OH) bending vibration; 1238 cm^{-1}, C–C stretching vibration; 1088 cm^{-1}, C–O stretching vibration; 918 cm^{-1}, CH2 stretching vibration; 833 cm^{-1}, C–C stretching vibration and C–H out-of-plane vibration.

Preprints (www.preprints.org) | NOT PEER-REVIEWED | Posted: 27 February 2023 doi:10.20944/preprints202302.0449.v1

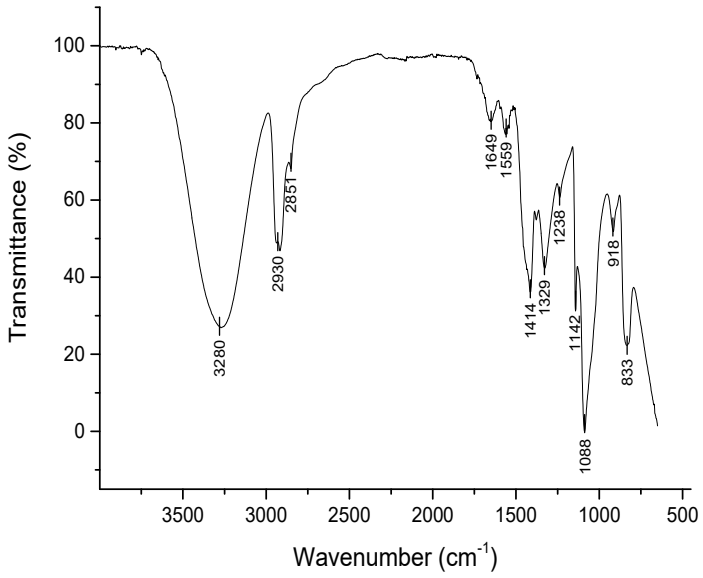

Figure 8. FTIR spectra of a PVA film produced by casting technique and irradiated with gamma rays at 25 KGy .

The band observed at 1142 cm^{-1} is associated to the stretching of C–O–C bond and can be an indicative of polymer crosslinking due to gamma irradiation [14]. According to the findings of Zainuddin et al. [30], it can be suggested that alkoxy radicals were formed in PVA chains (~CH2–CHO•–CH2~) when radiation reached the polymer. Then, these radicals underwent further transformations, leading to a formation of C–O–C bindings between mers within the same chain or those of different chains. These crosslinking reactions in PVA during radiolysis form a three-dimensional network of the hydrogel without the need of chemical crosslinking agent, that could induce cytotoxicity to the system.

Fig. 9 shows the FTIR spectra of samples loaded with MNZ. The spectrum TTNT + MNZ is very similar to that of samples after hydrothermal treatment (Fig.7), excepted by the presence of the absorption bands characteristic of MNZ, confirming the impregnation of MNZ in the titanate nanostructures. These MNZ bands were assigned to: anti-symmetric N-O and symmetrical elongation associated with the NO_2 group (1533 cm^{-1} and 1371 cm^{-1}, respectively); elongation N = O (1475 cm^{-1}); elongation C-O (1267 cm^{-1}); elongation C-N (1081 cm^{-1}); OH stretching (3214 cm^{-1}) [32,33]. A band at 877 cm^{-1} is also detected, which can be related both to the elongation of C-NO_2, characteristic of MNZ, and to the elongation of Ti-O, characteristic of titanate nanostructures.

On the contrary, absorption bands of MNZ or of titanate were not detected in FTIR spectra of samples coated with PVA (TTNT+MNZ+1PVA and TTNT+MNZ+6PVA), which suggested that MNZ molecules and titanate nanostructure were completely covered by PVA films, corroborating the contact angle analysis. Although spectrometer´s chamber was well purged by nitrogen, traces of gaseous carbon dioxide can be observed in some spectra. The double band at 2350 cm^{-1} presented in these spectra is assigned to asymmetric stretching modes of CO_2 [34].

Preprints (www.preprints.org) | NOT PEER-REVIEWED | Posted: 27 February 2023 doi:10.20944/preprints202302.0449.v1

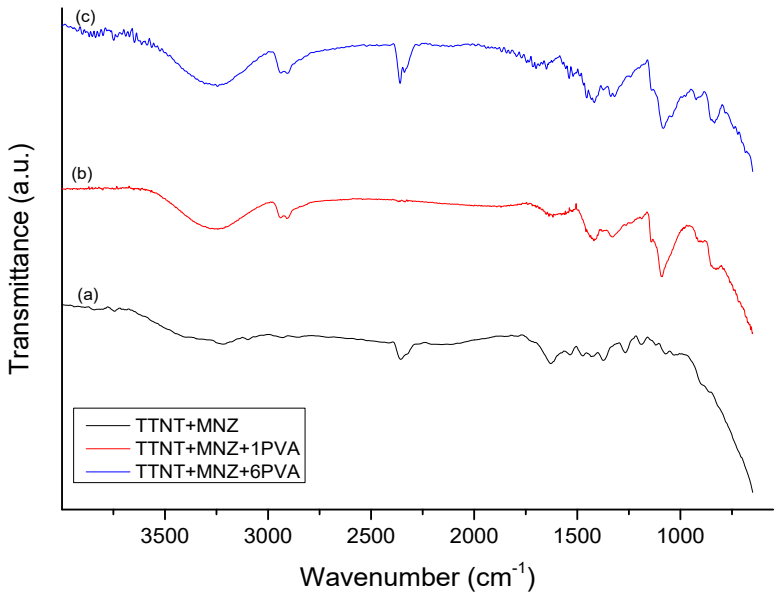

Figure 9. FTIR spectra of TTNT samples loaded with metronidazole: (a) TTNT+MNZ, (b) TTNT+MNZ+1PVA and (c) TTNT+MNZ+6PVA.

Fig.10 shows the FTIR spectra of samples after 14 days of immersion in PBS solution at 37 °C. In all spectra, large band centered at about 3250 cm^{-1} (-OH stretching) and band at 1637 cm^{-1} (H-O-H bending) can be visualized, although their intensity is higher in TTNT+MNZ+6PVA. These can be related to the –OH group stretching vibration of PVA and also to the absorption of water from PBS solution. Characteristic bands of PVA are clearly visualized in TTNT+MNZ+6PVA, while no characteristic vibration band of MNZ was identified. This could indicate the presence of the coating layer even after 14 days of immersion. As proposed before, probably a thick PVA coating acted as a strong physical barrier and obstructed the release of drug.

Preprints (www.preprints.org) | NOT PEER-REVIEWED | Posted: 27 February 2023 doi:10.20944/preprints202302.0449.v1

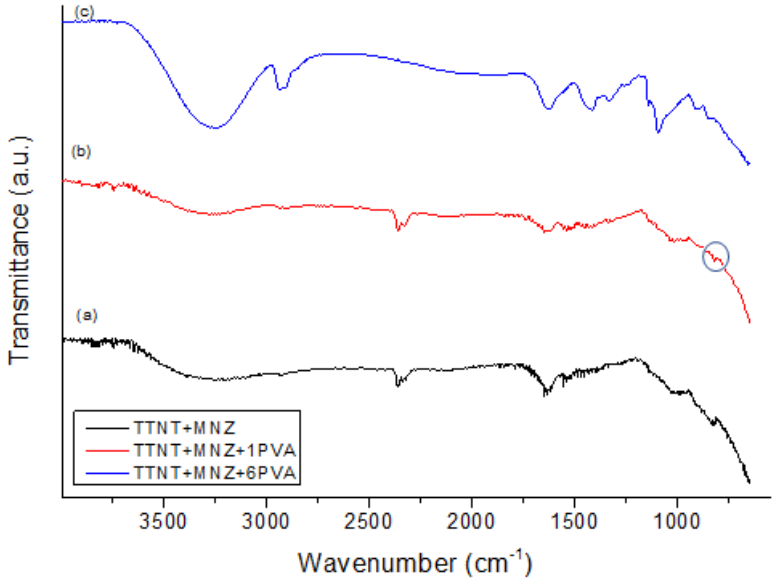

Figure 10. FTIR spectra of TTNT samples loaded with metronidazole, (a) TTNT+MNZ, and coated with PVA, (b) TTNT+MNZ+1PVA and (c) TTNT+MNZ+6PVA, after 14 days of immersion in PBS solution at 37 °C.

TTNT+MNZ and TTNT+MNZ+1PVA after MNZ release spectra (Fig.10 a,b) are very similar to that of pure TTNT (Fig.6), except by the presence of a small band at 1538 cm^{-1} that can be assigned to N-O antisymmetric stretching of MNZ molecules. In TTNT+MNZ spectrum, a shift in the band observed at 874 cm^{-1} (due to Ti-O stretching) to lower wavenumber (835 cm^{-1}), and consequently to lower energy, may be attributed to a formation of intermolecular interaction between TTNT and MNZ in aqueous environment. This shifted band was also observed in TTNT+MNZ+1PVA spectrum as a small shoulder (circled in Fig. 6b). This interaction can explain the partial release of MNZ molecules from these systems as proposed before, in item 3.3. The intense band at 1088 cm^{-1} related to C–O stretching vibration of PVA molecules was not present in TTNT+MNZ+1PVA spectra. It can be inferred that this layer of PVA in TTNT+MNZ+1PVA degraded in PBS solution at least in the sample region analyzed by FTIR.

To confirm this assumption, SEM was used to analyze the surface of the TTNT + MNZ + 1PVA group, before and after the "in vitro" metronidazole release assay (Figure 11). SEM image of the TTNT + MNZ + 1PVA before the release test (Fig.11a) shows a homogeneous coating of the PVA on the entire surface. The titanate nanostructure was not visualized due to the polymeric coating. The images after the MNZ release test (Fig.11b, c) reveal regions where the PVA coating has been degraded. In these regions, it is possible to observe tears in the polymeric coating and the morphology of the nanostructured film under the coating kept intact. This partial degradation of PVA film is in accordance with the FTIR results. Although PVA is soluble in water solution, most of its molecules remain insoluble due to the crosslinking, forming a hydrogel. Thus, the much higher content of MNZ released by TTNT + MNZ + 1PVA when compared to the system with 6 layers of PVA may be attributed to the erosion of the coating.

Preprints (www.preprints.org) | NOT PEER-REVIEWED | Posted: 27 February 2023 doi:10.20944/preprints202302.0449.v1

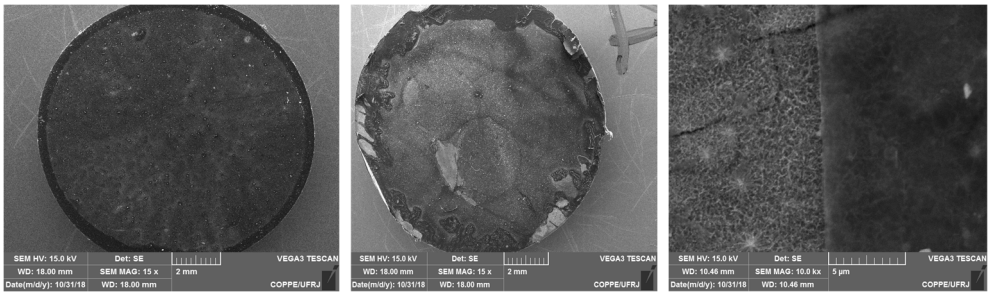

(a) (b) (c)

Figure 11. SEM images of TTNT + MNZ + 1PVA group, (a) before and (b,c) after "in vitro" MNZ release assay.

Although the thickness of the film affects its water uptake, a parallel between PVA cast film and PVA layer of TTNT + MNZ + 1PVA can be done. In order to estimate the water absorption capacity of the PVA layer on the Ti surface, a PVA hydrogel was produced by casting technique with 0.2 mm in thickness and irradiated with a dose of 25 KGy of gamma rays. This film showed a maximum absorption of 135% after 1 h of immersion in PBS pH 7.4 and reached an equilibrium swollen degree (stage in which the hydration forces are in equilibrium with crosslinking elastic forces) of 120% after approximately 24 h (data not shown). Based on this, the release of metronidazole from the TTNT + MNZ + 1PVA system may be related not only to the degradation of the coating, but also to the swollen of PVA layer due to the fluid absorption (swelling-induced mechanism), since the period of the achievement of MNZ constant release (Figure 6, Table 2) was coincident with the point of the maximum absorption of the PVA film.

The biological fluid uptake by systems coated with PVA provides hydrated environment that could facilitate the distribution of the antibiotic throughout the wound surgery site and contribute to wound healing in early stage.

4. Conclusions

In summary, the alkaline hydrothermal treatment successfully produced intertwined nanostructures like web on the titanium surface, presenting, in addition to good wettability and high bioactivity. With the aim of creating a local drug release device, the proposed surface modification strategy is simple, economical, and promising, since:

(1) It did not change the surface treatment and consequently the properties of the material;
(2) All groups reached the minimum inhibitory concentration to help fight bacteria and reduce the body's inflammatory response;
(3) All groups allowed an immediate delivery of metronidazole, which could reduce implant complications during the early wound healing processes;
(4) Although TTNT+MNZ showed higher percentage of antibiotic release within the studied groups, the PVA coating may absorb body fluids and water that provide distribution of MNZ throughout the wound surgery site, besides contributing to the hydration of the implant site, facilitating the wound healing;
(5) The design with 1 layer of PVA (TTNT + MNZ + 1PVA) showed to be the best option, since it can combine the water absorption capacity of the PVA-coated regions with the higher bioactivity of titanate nanostructure exposed in the degraded regions of the coating. Nevertheless, the effect of the crosslinking degree of PVA on the kinetic release of metronidazole should be better investigated.

The present study serves as proof that this method of surface modification can be a new alternative to the administration of systemic drugs, combining local antibiotic therapy with a surface treatment with proven efficacy. This delivery device could become a powerful approach to improve the integration of the titanium implant with the bone in dental applications, preventing early infections and bone failure. These results encourage further studies to evaluate the biological effectiveness of the proposed surface modification methodology.

Author Contributions: Conceptualization, P.M.J., I.R.S. and R.M.S.M.T.; methodology, I.R.S., R.S.S., A.T.S.B., J.N.L.; data curation, A.T.S.B., I.R.S., R.S.S., J.N.L., P.N.G.P..; writing—preparation of original draft, I.R.S., R.S.S., A.T.S.B.; writing—proofreading and editing, I.R.S., A.T.S.B., P.N.G.P, P.M.J., R.M.S.M.T.; project management, I.R.S., P.M.J., R.M.S.M.T.; financing acquisition, P.M.J, R.M.S.M.T. All authors have read and agreed to the published version of the manuscript.

Funding: The authors are grateful to the following Brazilian agencies: Coordenação de Aperfeiçoamento de Pessoal de Nível Superior—CAPES, National Council for Scientific and Technological Development - CNPq (Grant: 308789/2020-2), Fundação Carlos Chagas Filho de Amparo à Pesquisa do Estado do Rio de Janeiro - FAPERJ (Grant: Rede NanoSaúde—E-26/210.139/2019) for financial support.

Institutional Review Board Statement: Not applicable.

Data Availability Statement: The data presented in this study are available on request from the corresponding authors.

Acknowledgments: We acknowledge the Center of Nanotechnology Characterization at INT /SISNANO (CNPq-SisNANO 442604/2019–0)), the Multiuser Nucleus of Microscopy and the Multiuser Laboratory of Materials Characterization (LMCM), both at PEMM/COPPE/Federal University of Rio de Janeiro (UFRJ) for their support with the use of equipments.

Conflicts of Interest: The authors declare no conflict of interest. The funders had no role in the design of the study; in the collection, analyses, or interpretation of data; in the writing of the manuscript; or in the decision to publish the results.

References

1. Rupp, F.; Liang, L., Geis-Gerstorfer, J., Scheideler, L., & Hüttig, F. Surface characteristics of dental implants: A review. Dental Materials **2018**, 34(1), 40–57.
2. Lin L, Wang H, Ni M, Rui Y, Cheng T, Cheng C, Pan X, Li G, Lin C. Enhanced osteointegration of medical titanium implant with surface modifications in micro/nanoscale structures. Journal of Orthopaedic Translation **2014,** 2: 35 - 42.
3. Wang, Q., Zhou, P., Liu, S., Attarilar, S., Ma, R. L.-W., Zhong, Y., & Wang, L. Multi-Scale Surface Treatments of Titanium Implants for Rapid Osseointegration: A Review. Nanomaterials **2020**,10(6), 1244.
4. Oliveira, D.P.; Palmieri, A.; Carinci, F.; Bolfarini, C. Osteoblasts behavior on chemically treated commercially pure titanium surfaces. J Biomed Mater Res. **2014**,102(6): 1816-22.
5. Kang, B.; Lan, D.; Liu, L.; Dang, R.; Yao, C.; Liu, P.; Ma, F.; Qi, S.; Chen, X. Antibacterial Activity and Bioactivity of Zn-Doped TiO2 Coating for Implants. Coatings **2022**, 12,1264
6. Eggert, F.;Levin L. Biology of teeth and implants: The external environment, biology of structures, and clinical aspects. Quintessence Int. **2018**;49(4):301-312. doi:10.3290/j.qi.a38544
7. Kunrath, M. F.; Leal, B. F.; Hubler, R.; de Oliveira, S. D.; Teixeira, E. R. Antibacterial potential associated with drug-delivery built TiO2 nanotubes in biomedical implants. AMB Express **2019**, 9(1).
8. Pecoraro, C.; Carbon; D., Deng, D.; Cascioferro, S. M.; Diana, P.; Giovannetti, E. Biofilm Formation as Valuable Target to Fight against Severe Chronic Infections. Current Medicinal Chemistry **2022**, 29(25), 4307-4310.
9. Li, Z.; Xu, W.; Wang, X.; Jiang, W.; Ma, X.; Wang, F.; et al. Fabrication of PVA/PAAm IPN hydrogel with high adhesion and enhanced mechanical properties for body sensors and antibacterial activity. European Polymer Journal **2021**, 146, 110253.
10. Ebhodaghe, O. S. Hydrogel – based biopolymers for regenerative medicine applications: a critical review. International Journal of Polymeric Materials and Polymeric Biomaterials **2022**, 71(3), 155-172.
11. Rivera-Hernández, G.; Antunes-Ricardo, M.; Martínez-Morales, P.; Sánchez, M. L. Polyvinyl alcohol based-drug delivery systems for cancer treatment. International Journal of Pharmaceutics **2021**, 600, 120478.
12. Muthuraj, M. S. A. Antimicrobial Susceptibility of Periodontopathogens. Clinical Dentistry **2021**, (0974-3979), 9(7).
13. Dilley, M.; Geng, B. Immediate and delayed hypersensitivity reactions to antibiotics: aminoglycosides, clindamycin, linezolid, and metronidazole. Clinical Reviews in Allergy & Immunology **2022,** 62(3), 463-475.

14. Oliveira, R. N.; Rouze, R.; Quilty, B.; Alves, G. G.; Soares, G. D. A.; Thire, R. M. S. M.; McGuinness, G. B. Mechanical properties and in vitro characterization of polyvinyl alcohol-nano-silver hydrogel wound dressings. Interface Focus **2013**, 4(1), 20130049–20130049.
15. Da Silva, M. A. C.; Membranas bioreabsorvíveis de Poli(3- Hidroxibutirato) carregadas com metronidazol para regeneração tecidual guiada. Doctoral thesis, Universidade Federal do Rio de Janeiro, Rio de Janeiro, Brazil, 2014.
16. Anitha, V. C.; Banerjee, A. N.; Joo, S. W.; Min, B. K. Morphology-dependent low macroscopic field emission properties of titania/titanate nanorods synthesized by alkali-controlled hydrothermal treatment of a metallic Ti surface. Nanotechnology **2015** , 26(35), 355705.
17. Manivasagam, V. K.; Popat, K. C. Hydrothermally treated titanium surfaces for enhanced osteogenic differentiation of adipose derived stem cells. Materials Science and Engineering: C **2021**, 128, 112315.
18. Kokubo, T.; Matsushita, T.; Takadama, H.; Kizuki, T. Development of bioactive materials based on surface chemistry. Journal of the European Ceramic Society **2009**, 29(7), 1267–1274.
19. Huang, Y. Z.; He, S. K.; Guo, Z. J.; Pi, J. K.; Deng, L.; Dong, L. et al. Nanostructured titanium surfaces fabricated by hydrothermal method: influence of alkali conditions on the osteogenic performance of implants. Materials Science and Engineering: C **2019**, 94, 1-10.
20. Bright, R.; Hayles, A.; Wood, J.; Ninan, N.; Palms, D.; Visalakshan, R.M.; Burzava, A.; Brown, T.; Barker, D.; Vasilev, K. Bio-Inspired Nanostructured Ti-6Al-4V Alloy: The Role of Two Alkaline Etchants and the Hydrothermal Processing Duration on Antibacterial Activity. Nanomaterials **2022**,12,1140.
21. Morgado, E.; De Abreu, M. A. S.; Pravia, O. R. C. et al. A study on the structure and thermal stability of titanate nanotubes as a function of sodium content. Solid State Sciences **2006**, 8 (8), 888-900.
22. Scarano, A.; Rexhep, S.T.; Lorusso, F.; Leo, L. Wettability of implant surfaces: Blood vs autologous platelet liquid (APL), Journal of the Mechanical Behavior of Biomedical Materials **2021**. doi: https://doi.org/10.1016/j.jmbbm.2021.104773.
23. Hosseini, S.H.; Kazemian,M.; Ghorbanzadeh, S. A brief overview of cellular and molecular mechanisms of osseointegration. Int J Contemp Dent Med Rev **2015**, Article ID: 010415.
24. Terheyden, H.; Lang, N.P.; Bierbaum, S.; Stadlinger, B. Osseointegration – communication of cells. Clin Oral Implants Res. **2012,** 23(10):1127-1135. doi:10.1111/j.1600-0501.2011.02327.x
25. He, Y.; Gao, Y.; Ma, Q.; Zhang, X.; Zhang, Y.; Song, W. Nanotopographical cues for regulation of macrophages and osteoclasts: emerging opportunities for osseointegration. Journal of Nanobiotechnology **2022**, 20(1), 1-22.
26. Ferencík, M.; Rovensky, J.; Matha, V.; & Herold, M. Kompendium der Immunologie: Grundlagen und Klinik. Springer-Verlag **2006**.
27. Poulet, P. P.; Duffaut, D.; Lodter, J. P. Metronidazole susceptibility testing of anaerobic bacteria associated with periodontal disease. Journal of Clinical Periodontology **1999**, 26(4), 261–263.
28. Yoshida, R.; Suzuki, Y.; & Yoshikawa, S. Syntheses of TiO2(B) nanowires and TiO2 anatase nanowires by hydrothermal and post-heat treatments. Journal of Solid State Chemistry **2005**, 178(7), 2179–2185.doi:10.1016/j.jssc.2005.04.025
29. Xie, J.; Wang, X.; & Zhou, Y. (2012). Understanding Formation Mechanism of Titanate Nanowires through Hydrothermal Treatment of Various Ti-Containing Precursors in Basic Solutions. Journal of Materials Science & Technology, 28(6), 488–494.doi:10.1016/s1005-0302(12)60087-5
30. Lin, L.; Wang, H.; Ni, M.; Rui, Y.; Cheng, T.-Y.; Cheng, C.-K.; … Lin, C. (2014). Enhanced osteointegration of medical titanium implant with surface modifications in micro/nanoscale structures. Journal of Orthopaedic Translation, 2(1), 35–42.
31. Zainuddin, Hill, D. J. T.; Le, T. T. An ESR study on γ-irradiated poly(vinyl alcohol). Radiation Physics and Chemistry **2001**, 62(2-3), 283–291.
32. Herculano, R. D.; Guimarães, S. A. C.; Belmonte, G. C.; Duarte, M. A. H.; Oliveira Júnior, O. N. de, Kinoshita, A.; Graeff, C. F. de O. Metronidazole release using natural rubber latex as matrix. Materials Research **2010**, 13(1), 57–61.
33. Brako, F.; Luo, C.; Matharu, R. K.; Ciric, L.; Harker, A.; Edirisinghe, M.; Craig, D. Q. M. A Portable Device for the Generation of Drug-Loaded Three-Compartmental Fibers Containing Metronidazole and Iodine for Topical Application. Pharmaceutics **2020**, 12(4), 373.
34. Pavia, D. L.; Lampman, G. M.; Kriz, G. S.; Vyvyan, J. A. Introduction to spectroscopy. Cengage learning, **2014.**